Activin A activation of Smad3 mitigates innate inflammation in mouse models of psoriasis and sepsis

Thierry Gauthier[1], Yun-Ji Lim[1], Wenwen Jin[1], Na Liu[1], Liliana C. Patiño[1], Weiwei Chen[1], James Warren[2], Daniel Martin[3], Robert J. Morell[3], Gabriela Dveksler[2], Gloria H. Su[4], WanJun Chen[1,*]

[1]Mucosal Immunology Section, National Institutes of Dental and Craniofacial Research (NIDCR), National Institutes of Health, Bethesda, Maryland, USA

[2]Uniformed Services University, Department of Pathology, Bethesda, Maryland, USA

[3]Genomics and Computational Biology Core, National Institute on Deafness and Other Communication Disorders, National Institutes of Health, Bethesda, Maryland, USA

[4]Department of Pathology and Cell Biology, Columbia University Irving Medical Center, New York, NY, USA

*Correspondence should be addressed to W.J.C (wchen@mail.nih.gov), 30 convent Drive, 20892, Bethesda, MD, United States. Phone number: 301-435-7168

Abstract

Phosphorylation of Smad3 is a critical mediator of TGF-β signaling, which plays an important role in regulating innate immune responses. However, whether Smad3 activation can be regulated in innate immune cells in TGF-β-independent contexts remains poorly understood. Here, we show that Smad3 is activated through the phosphorylation of its C-terminal residues (pSmad3C) in murine and human macrophages in response to bacterial and viral ligands, which is mediated by Activin A in a TGF-β independent manner. Specifically, infectious ligands, such as LPS, induced secretion of Activin A through the transcription factor STAT5 in macrophages, and Activin A signaling in turn activated pSmad3C. This Activin A-Smad3 axis controlled the mitochondrial ATP production and ATP conversion into adenosine by CD73 in macrophages, enforcing an anti-inflammatory mechanism. Consequently, mice with a deletion of Activin A receptor 1b specifically in macrophages (*Acvr1b*$^{f/f}$*-Lyz2cre)* succumbed more to sepsis due to uncontrolled inflammation and exhibited exacerbated skin disease in a mouse model of imiquimod-induced psoriasis. Thus, we have revealed a previously unrecognized natural brake to inflammation in macrophages that occurs through the activation of Smad3 in an Activin A-dependent manner.

Introduction

Macrophages are crucial for the mount of a proper immune response. Their activation and polarization toward a pro-inflammatory phenotype enable them to clear pathogens and protect our body during infections (1, 2). However, they need intrinsic brakes to avoid overt-inflammation, tissue damage, and promote the resolution and return to homeostasis (3-6). A way for innate immune cells to avoid overt-inflammation is to produce anti-inflammatory cytokines such as IL-10 (Interleukin-10) and TGF-β1 (Transforming Growth Factor-β1) (7, 8). TGF-β1 belongs to the TGF-β superfamily of proteins which is composed of TGF-βs, Activins, Nodal, GDFs (Growth Differentiation Factor) and BMPs (Bone Morphogenic Proteins). TGF-β, after binding to its receptors, signals through a canonical pathway involving the Smad proteins. TGF-β promotes the phosphorylation of Smad3 in its C terminal domain (Serine 423 and 425, hereafter called pSmad3C) which induces the translocation of Smad3 to the nucleus and its binding onto the promoter of its target genes (9-11). This TGF-β-Smad3 axis has been described to be active in macrophages and to regulate inflammation (12, 13). It has also been described that LPS could transactivate the TGF-βRI via TLR4 (Toll Like Receptor 4) suggesting that the TGF-β signaling could be regulated by inflammatory stimuli (14). However, whether Smad3 can be activated by other stimuli than TGF-β, especially in the context of inflammatory-mediated environments remains poorly understood.

Here, we discovered that bacterial and viral ligands such as LPS (Lipopolysaccharide) can induce pSmad3C in an Activin A-dependent, but TGF-β-independent manner. LPS activated a pathway linked to MEK/ERK kinases and STAT5 to promote the expression of the gene encoding Activin A (*Inhba*) and its receptors. Activin A induced pSmad3C *in vitro* and *in vivo* in inflammatory

models of sepsis and psoriasis, and importantly also in human macrophages. We determined that this Activin A-Smad3 axis was a natural brake to inflammation which prevented the overt-activation of macrophages in response to inflammatory stimuli, and suppressed inflammation in experimental sepsis and psoriasis. Thus, our findings shed lights on a previously unrecognized natural brake to inflammation in macrophages that occurs by the activation of Smad3 in an Activin A-dependent manner.

Results

LPS induces pSmad3C in a TGF-β independent manner *in vitro*

It is well known that TGF-β signaling activates the transcription factor Smad3 through phosphorylation in innate and adaptive immune cells (12, 15, 16). However, we unexpectedly discovered that LPS induced Smad3 phosphorylation in its C terminal domain (Serine 423/425, hereafter referred as pSmad3C) in murine macrophages. Specifically, LPS-induced pSmad3C started 4 h after treatment, peaked at 6h and stayed stable until 24 h in *in vitro* cultures (**Fig 1A and S1A, Western blotting quantifications are presented in Fig S12 and S13**), whereas the levels of total SMAD3 protein were largely unaltered (except for a reduction at 24 h suggesting a negative retro-control mechanism) (**Fig 1A**). Smad3 phosphorylation can also occur in the linker region (Serine 213 and Tyrosine 179) in response to TGF-β and/or other factors (17), however, LPS was unable to induce Smad3 phosphorylation in these sites in the linker region (**Fig S1A, and data not shown**), suggesting the specificity of C-terminal phosphorylation of Smad3. The fact that Smad3 was not phosphorylated until 4 h after LPS treatment suggested that pSmad3C was induced *via* the synthesis of new proteins rather than through a direct LPS-mediated signaling. Indeed, the translation inhibitor cycloheximide completely abrogated pSmad3C confirming the requirement of new protein synthesis (**Fig 1B**). Since TGF-β1 is the primary inducer of pSmad3C, we initially hypothesized that LPS induced pSmad3C by promoting the production of TGF-β and/or enhancing its signaling, which in turn acted in a paracrine or autocrine manner. We first determined that the *Tgfb1* mRNA was not upregulated until 6 h after LPS treatment, which was later than the appearance of pSmad3C at 4 h (**Fig S1B**). Importantly, we blocked the TGF-β signaling by using the specific antibody 1D11 that

neutralizes TGF-β 1, 2 and 3 in wild-type macrophages (**Fig 1C, S1C**)(18, 19) or by using macrophages from RI-Lyz2 cre mice (*Tgfbr1* $^{flox/flox}$ crossed with Lyz2cre^{+} mice)(12) in which *Tgfbr1* was deleted specifically in macrophages (**Fig 1D, S1D**), and treated these macrophages with LPS to measure pSmad3C. In all aforementioned conditions, the pSmad3C induction by LPS was unchanged compared to their respective wildtype controls, while the TGF-β induction of pSmad3C was abrogated as expected (**Fig 1C and D**). These data collectively demonstrate that LPS induces pSmad3C in a manner independent of TGF-β signaling.

Macrophages induce pSmad3C in LPS -or CLP-induced sepsis in mice independently of TGF-β

We next investigated if Smad3 could be phosphorylated *in vivo* during LPS-induced endotoxin shock and CLP (Cecal Ligation Puncture)-induced sepsis in mice. In line with our *in vitro* data, intraperitoneal injection of LPS induced a dramatic increase in pSmad3c in peritoneal cells (**Fig 1E**). On the other hand, the levels of pSmad3 Ser213 in the Smad3 linker region were not upregulated, and the levels of pSmad3 Tyr179 were not detected in all the samples (data not shown) confirming the specific activation of pSmad3C upon LPS stimulation. Among the peritoneal cells, we observed that macrophages were the main population in which pSmad3C was significantly increased after LPS treatment (**Fig 1F, see Fig S1E for gating strategy**). Importantly, the induction of pSmad3C remained unaffected in RI-Lyz2cre mice indicating that TGF-β is indeed dispensable for Smad3 activation in response to LPS (**Fig 1G**). Strikingly, a similar phenomenon was observed during CLP-induced sepsis (**Fig 1H and I, Fig S1F**). The data collectively confirm that LPS induces pSmad3C in a TGF-β independent manner *in vivo* during sepsis.

LPS activation of Smad3 requires Activin A in murine and human macrophages

We next determined the mechanisms by which LPS induces pSmad3C. To address this, we first performed RT-qPCR on the genes related to the TGF-β superfamily of proteins in macrophages. We observed that the levels of *Smad2*, *Smad3*, *Bambi* and *Acvr2b* were not significantly changed after LPS treatment (**Fig S2A**). The expression of the inhibitory Smads, e.g *Smad6* and *Smad7*, were decreased after 2 h of LPS treatment but this effect was transient (**Fig S2A**). We also did not detect any expression of *Inha* and *Inhbb* (both encoding subunits of Inhibin). However, starting at 2 h after LPS treatment and peaking at 6 h, the levels of the Activin A receptors *Acvr2a* and *Acvr1b* expression were significantly increased. Strikingly, the mRNA of *Inhba* (encoding Activin A) and the protein levels of Activin A were both markedly increased with a peak at 6 h (**Fig 2A and B**). Interestingly, *Inha*, *Inhbb* and *Acvr1c* (which are other molecules associated with the Activin signaling) were not expressed in macrophages (data not shown). This suggests a role of Activin A in the phosphorylation of Smad3 in response to LPS. Indeed, blockade of the Activin A effect by using the natural Activin A inhibitor Follistatin or an Activin A-blocking antibody completely abrogated the pSmad3C induced by LPS (**Fig S3A**). We also confirmed that the blocking antibody indeed blocked the ability of Activin A to induce pSmad3C (**Fig S3B**). To further confirm this, we next generated *Acvr1b*-Lyz2cre mice by crossing *Acvr1b*$^{flox/flox}$ mice with Lyz2cre^{+} mice to study the effect of Activin A receptor deletion on pSmad3C in macrophages (20). We first confirmed that the recombination between *Acvr1b* and Lyz2 cre was efficient (**Fig S3C**) and that the Activin A signaling (and its ability to induce pSmad3C) was blocked in *Acvr1b*-Lyz2 cre macrophages (**Fig S3D**), altogether confirming the deletion of *Acvr1b*. We also showed that pSmad3C was completely abrogated in these knockout

macrophages in response to LPS (**Fig 2C**), confirming that the Activin A signaling is indeed responsible for Smad3 phosphorylation. Importantly, *INHBA* (encoding human ACTIVIN A) expression was also induced after LPS treatment in human macrophages (**Fig 2D**), and the induction of pSMAD3C by LPS was abolished by Activin A blockade while the inhibition of TGF-β did not affect it (**Fig 2E**).

Having elucidated that LPS-induced pSmad3C occurs through Activin A in macrophages *in vitro*, we next showed that intraperitoneal injection of LPS (endotoxin model) or CLP-surgery (sepsis model) induced a significant increase in Activin A protein in the blood of mice (**Fig 2F and G**). In macrophages, we observed that the induction of pSmad3C was abrogated in *Acvr1b*-Lyz2cre mice indicating that Activin A is indeed indispensable for Smad3 activation in sepsis models induced by LPS and CLP-surgery (**Fig 2H and I**). Thus, the LPS induction of pSmad3C is dependent on Activin A signaling in both murine and human macrophages.

The Activin A-SMAD3 axis restrains LPS-induced inflammation in macrophages

We next investigated the function of the Activin A-Smad3 axis in macrophages. Blockade of Activin A or its downstream target Smad3 resulted in enhanced mRNA expression of pro-inflammatory cytokines including *Tnf*, *Il6*, *Cxcl9* and *Il27,* but decreased anti-inflammatory genes *Tgfbi* and *Arg1* (**Fig 2J and K and S3E-G**). Importantly, this axis is specific for some genes since *Il1b* was not affected by *Smad3* or *Acvr1b* deletions, and *Il10* was only affected by *Acvr1b* deletion (suggesting additional effects of Activin A that might be independent of Smad3) (**Fig S3F and G**). Consistently, blockade of Activin A also significantly increased the protein levels of TNF-α and IL-6 in macrophage treated by LPS (**Fig S3H**). Importantly, human macrophages

treated by LPS in the presence of Follistatin or anti-Activin A antibody exhibited significantly higher levels of *Il6* expression compared to LPS-treated macrophages alone (**Fig 2L**). Similarly, inhibition of Smad3 function (by using a Smad3 inhibitor) also increased the expression of *IL6* in human macrophages (**Fig 2M**).

We then further determined that Smad3 was signaling downstream of Activin A to decrease inflammation. We showed that the inhibition of Smad3 with its specific inhibitor blocked the Activin A induced suppression of *Il6* gene expression in normal macrophages (**Fig S3I**). In addition, *Smad3* KO macrophages exhibited a severe defect in the suppression of *Il6* and *Tnfa*, and an increase in *Tgfbi* in response to Activin A treatment, when compared with wild type macrophages (**Fig 2N**). The data collectively indicates that Activin A-mediated pSmad3C controls inflammatory cytokines in macrophages in response to LPS.

LPS induces the Activin A-pSmad3C axis through STAT5

Next, we deciphered the signaling pathway leading to Activin A expression and consequent Smad3C phosphorylation in response to LPS. We first observed that this axis was dependent on TLR4 and MyD88 (Myeloid differentiation primary response 88) since macrophages deficient for these genes exhibited severely deficient *Inhba* expression and decreased Smad3C phosphorylation in response to LPS (**Fig 3A-C**). However, macrophages with deficient TRIF (encoded by *Ticam1*) (TIR-domain-containing adapter-inducing interferon-β) showed normal pSmad3C upon LPS stimulation, suggesting that TRIF is dispensable to activate the Activin A-Smad3 pathway by LPS (**Fig S4A**). As TRAF6 (TNF receptor associated factor 6) is a key molecule downstream of MyD88, and a crucial activator of TAK1 (Transforming growth factor-β-activated

kinase 1) (21), we next examined the function of TRAF6 and TAK1 in LPS-induced Activin A-pSmad3C. We first showed that macrophages deficient in *Traf6* (*Traf6*-Lyz2cre) expressed markedly reduced *Inhba* mRNA and pSmad3C (**Fig 3D and E**). Similarly, suppression of TAK1 activity with its specific inhibitor also significantly decreased the *Inhba* gene expression and substantially blocked pSmad3C induced by LPS (**Fig 3F and G**), suggesting a critical role of TRAF6-TAK1 in this pathway (**Fig 3D-G**). Finally, we determined that the MAP kinases, MEK and ERK, which have been described to be downstream molecules of TRAF6 and TAK1 in the LPS signaling cascade were crucial for the axis (21), because inhibition of MEK (MAP kinase kinase) and ERK (Extracellular signal-regulated kinases) activity abolished LPS-induced expression of activin A and consequentially the pSmad3C induction (**Fig 3H and I**).

We next searched for the transcription factor(s) that could be regulated by this TLR4-MyD88-TRAF6/TAK1-MEK/ERK pathway. We first observed that the transcription factor STAT5 possessed some predicted binding sites into the *Inhba* promoter, suggesting that STAT5 could be responsible for the induction of *Inhba* expression (**Fig S4B**). We then demonstrated that STAT5 was phosphorylated after LPS treatment in a timeline that was consistent with the induction of *Inhba* expression (less than 2 h after LPS treatment) while the expression of total *Stat5a* and *Stat5b* mRNA remained unchanged (**Fig 3J and S4C**). Of importance, the phosphorylation of STAT5 was dependent on TRAF6, TAK1, MEK and ERK, as blockade of each of these molecules substantially inhibited the STAT5 activation (**Fig S4D and S4E**). At the molecular level, we found that the binding of STAT5 to several sites at the *Inhba* promoter was significantly increased at 3 h after LPS treatment (**Fig 3K**). Importantly, STAT5 inhibition in wild-type macrophages or the use of *Stat5*-Lyz2 cre macrophages abrogated both the expression of

Inhba and pSmad3C induced by LPS (**Fig 3L-O**). The validation of the different proteins knock-down and inhibitors selectivity from Figure 3 is presented in **Fig S5**). Thus, the data collectively reveal that STAT5 activation plays a key role in LPS-induced Activin A production and pSmad3C activation.

The Activin A-Smad3 axis controls ATP metabolism

To understand the mechanisms underlying this Activin A-Smad3 function in response to LPS-induced inflammation, we performed RNAseq analysis on macrophages from WT or *Smad3* KO mice treated with LPS for 24 h. *Smad3* KO macrophages exhibited a largely remodeled phenotype with 1444 genes up-regulated and 1216 down-regulated compared to WT macrophages (**Fig S6A**). Analysis of the pathways up- and down-regulated showed that *Smad3* KO macrophages had a large increase in pro-inflammatory pathways (for example response to virus, regulation of defense response, cell activation etc) while the down-regulated pathways were largely enriched in metabolic pathways (metabolism of lipids, carbohydrate metabolic pathway, metabolism of carbohydrate etc) (**Fig S6B**) suggesting that the Activin A-Smad3 pathway regulates macrophages immunometabolism in response to LPS.

Among the metabolic genes regulated by Smad3, several related to mitochondria metabolism and functions were downregulated (**Fig 4A**). Since mitochondria is a critical hub to regulate macrophage immunometabolism (22-24), we next investigated whether the Activin A-pSmad3C pathway regulated mitochondrial functions in response to LPS. Interestingly, we observed that when *Smad3* KO or *Acvr1b*-Lyz2 cre macrophages treated with LPS were stained with the Mitotracker green to quantify mitochondria, these KO macrophages had decreased

mitochondrial numbers compared to WT macrophages (**Fig 4B and C, S7A and B**). However, the levels of mitochondrial membrane potential (φm) and mitochondrial ROS (reactive oxygen species) were similar between the *Smad3* KO and WT macrophages (**Fig S7C**). Similarly, WT macrophages treated with Follistatin or anti-Activin A antibody had decreased levels of mitochondria but unchanged levels of φm and mROS (**Fig S7D and E**). One of the critical functions of mitochondria is to generate energy via the production of ATP. Indeed, *Smad3* KO and *Acvr1b*-Lyz2 cre macrophages had also decreased ATP levels (**Fig 4D and E**). Given the critical role of ATP in regulating cellular functions (25), we reasoned that restoring the levels of ATP by supplementing exogenous ATP (at low amounts to avoid inflammasome activation and cell death) in the culture would reverse the pro-inflammatory phenotype observed in *Smad3* KO and *Acvr1b*-Lyz2cre macrophages. Indeed, we found that the levels of *Arg1* and *Tgfbi* were significantly increased after ATP treatment in these knockout macrophages (**Fig 4F and G**). Similar increases in *Arg1* and *Tgfbi* were also observed in Follistatin treated wild type macrophages (**Fig S7F**). These results demonstrate that the disruption of the Activin A-Smad3 axis dysregulates ATP production, which regulates the expression of *Arg1* and *Tgfbi* in LPS activated macrophages. Importantly, most of these changes are the reflection of the Activin A-Smad3 axis activation during LPS-induced inflammation since they could not be observed in macrophages in absence of LPS stimulation (**Fig S8A-E**).

A way for ATP to decrease inflammation is to be converted to adenosine by the ectonucleotidases CD39 and CD73, leading to the activation of the transcription factor CREB (26, 27). Of note, while the expression of *Entpd1* (encoding CD39) was increased in *Acvr1b*-Lyz2 cre macrophages, the expression of *Nt5e* (encoding CD73) was dramatically decreased in both

Acvr1b-Lyz2 cre and *Smad3* KO macrophages (**Fig 4H and S7G**). In addition, while *Acvr1b*-Lyz2 cre or *Smad3* KO macrophages treated with LPS reinforced their expression of *Arg1* and *Tgfbi* in the presence of ATP, this effect was totally abrogated when CD73 or CREB activities were inhibited (**Fig 4I and J**). Furthermore, the same result was obtained in WT macrophages treated with Follistatin (**Fig S7H**). Finally, we observed that wild type macrophages treated with a combination of LPS and Activin A increased expression of *Nt5e,* which was completely abrogated in *Smad3* KO macrophages (**Fig S7I**). The data suggest that, in addition to its direct binding to the loci of several inflammatory genes, Smad3 also indirectly restricts inflammation by modulating ATP metabolism, and its degradation into adenosine by CD73, which consequently activates the transcription factor CREB (**Fig S7J**).

Activin A-mediated Smad3 activation suppresses sepsis

Having elucidated that LPS-induced pSmad3C through the Activin pathway acts as a negative regulator for macrophage activation *in vitro* and *in vivo,* we next investigated whether this regulated inflammation in mice. For this, we first utilized the LPS induced endotoxin shock in mice. In this model, *Acvr1b*-Lyz2 cre mice succumbed more and faster to the disease (**Fig 5A**). This was linked to a higher level of the inflammatory cytokine IL-6 (**Fig 5B, S9A**). The observation that IL-6 levels were already elevated early (1-3 h) after LPS injection suggests that the heightened inflammation is unlikely to be caused by secondary activation of neutrophils (**Fig S9A**). We next used a CLP- induced model of sepsis (in which real infection occurs) to confirm our findings. In this sepsis model, *Acvr1b*-Lyz2 cre mice also had lower survival rates and increased levels of inflammation (**Fig 5C and D**). Similarly, *Smad3* KO mice also had lower survival rates after LPS injection or CLP-surgery combined with higher levels of pro-

inflammatory cytokines (**Fig S9B-E**), which is consistent with a previous report (28). Overall, the Smad3 activation by Activin A suppresses the development of sepsis in mice.

We then extended our studies to human patients to interrogate whether this Activin A-pSmad3C axis was also activated in human patients with sepsis. For this, we analyzed a cohort of sepsis patients that was already published in the Single Cell portal from the Broad Institute (29). Interestingly, the expression of *Inhba*, *Smad3*, *Acvr1b*, *Acvr2a*, *Stat5a* and *Stat5b* were all higher in the macrophages of patients compared to healthy volunteer (**Fig S9F**), suggesting that the Activin A-Smad3-STAT5 axis is also involved in human sepsis.

SARS-Cov2 viral E protein activates Activin A-Smad3 pathway in macrophages

Patients severely affected by SARS-Cov2 infection develop a disease resembling sepsis in which the virus trigger activation of the innate immune system and generates inflammation (30, 31). We therefore hypothesized that the Activin A-Smad3 pathway might be activated during inflammation induced by viral ligands such as SARS-CoV2. To study this, we used the E protein from SARS-CoV2 which has been described to be the mediator of inflammation during this viral infection in a TLR2-dependent pathway (32). We firstly took the advantage that murine macrophages can be activated by E protein (12, 32) and stimulated macrophages *in vitro* with E protein to examine the expression of *Inhba* and the phosphorylation of Smad3. We found that E protein indeed induced significant increase in Activin A and the phosphorylation of Smad3C in an ACVR1B dependent manner (**Fig S10A and B**). Importantly, human macrophages also exhibited higher levels of *INHBA* expression and increased pSMAD3C in an Activin A dependent manner in response to E protein challenge (**Fig S10C and D**). Similarly to LPS stimulation, E

protein stimulation of wild-type macrophages in which Activin A signaling was blocked or *Smad3* KO macrophages resulted in much higher levels of inflammatory cytokines compared to WT macrophages (**Fig S10E and F**). These findings indicate that the Activin A-Smad3 axis also restrains viral-induced inflammation and possibly sepsis, such as the one occurring during Covid-19 infection.

Activin A-mediated Smad3 activation regulates psoriatic inflammation

We observed that pathogen associated molecular patterns (e.g. bacterial LPS and viral E protein) that can be sensed in the extracellular environment by plasma membrane receptors (TLR 4 and 2, respectively) triggers the production of Activin A and consequent activation of Smad3 to restrain overt-inflammation. However, whether TLR ligands that signal through endosomal receptors could do the same remains poorly understood. We therefore used the TLR7 ligand imiquimod (IMQ) to test if that was the case. We observed that, similarly to LPS, IMQ promoted *Inhba* expression in a manner dependent on TAK, MEK, ERK and STAT5 as well as TLR7 and MyD88 in macrophages in culture (**Fig 6A and S11A**). Similarly, IMQ induced pSmad3C in an Activin A dependent manner since deletion of *Acvr1b* in macrophages abrogated IMQ effect (**Fig 6B**). Importantly, the same results were obtained in human monocytes (**Fig 6C and D**), namely IMQ enhanced *INHBA* expression and pSmad3C, and blockade of ACTIVIN A signaling abolished the IMQ effects. As expected, *Smad3* KO and *Acvr1b*-Lyz2 cre macrophages were hyper-inflammatory upon IMQ treatment in vitro (**Fig 6E and F, S11B**).

We next used the IMQ-induced psoriasis model in mice (33) to study the role of the Activin A-Smad3 pathway in macrophages in the regulation of the disease. We observed that, 6h after

IMQ application on the skin, the levels of *Inhba* and pSmad3C were significantly increased in the skin tissue (**Fig 6G and H**). We then interrogated the role of this signaling cascade to the development of psoriasis. To avoid any potential impact on other cells expressing Smad3, we intradermally injected WT or *Smad3* KO macrophages ($CD45.2^+$) into the back skin of CD45.1 WT mice followed by IMQ application daily on the skin for 6 days. Transfer of *Smad3* KO macrophages had a deleterious effect on the disease, marked by an increase in skin thickness and an increased production of pro-inflammatory cytokines by γδ T cells which are the main drivers of the disease (33) (**Fig 6I and J, S11C**). To provide further evidence that *Smad3* deficient macrophages could be inflammatory in an endogenous context as well upon IMQ treatment, we generated bone marrow chimeras (BM chimeras) by reconstituting lethally irradiated CD45.1 mice with BM from CD45.2 WT or *Smad3* KO mice. We observed an almost complete reconstitution of the immune system in the blood (**Fig S11D**) and about 60 % of macrophages reconstitution in the skin of both WT and *Smad3* KO BM chimeras (**Fig S11E**). Interestingly, upon IMQ application, *Smad3* KO BM chimeras had exacerbated psoriasis development as exemplified by increased skin thickness (**Fig S11F and G**). This was associated with an increased ability of the reconstituted macrophages to produce IL-6 (**Fig S11H**) confirming that *Smad3* deficient macrophages are indeed pro-inflammatory in the context of psoriasis. In addition, *Acvr1b*-Lyz2cre mice also developed more severe disease compared to wild-type mice (**Fig 6K, S11I**), which was associated with an increased infiltration of macrophages in the skin, and more IL-6 and TNF-α producing macrophages (**Fig 6L and M**). γδ T cells also produced more pro-inflammatory cytokines (e.g IL-17A, IL-22 and IFN-γ) in *Acvr1b*-Lyz2 cre mice (**Fig 6N**). We then deciphered how macrophages regulated the disease development and γδ T cells activation.

Since *Acvr1b*-Lyz2 cre macrophages produced more pro-inflammatory cytokines, we hypothesized that the Activin A-Smad3 pathway in macrophages might regulate γδ T cell activation and the disease by regulation of the cytokine production in macrophages. We thus blocked the pro-inflammatory cytokines TNF-α, IL-6, IL-1β and IL-23A, which have been known to be crucial to γδT cell activation, in WT and *Acvr1b*-Lyz2 cre mice during psoriasis. We observed that the increased skin thickness and γδ T cells activation in *Acvr1b*-Lyz2 cre mice were abrogated when these pro-inflammatory cytokines were blocked (**Fig S11J**). The data indicate that activin A mediated Smad3 phosphorylation also restrain macrophage activation during psoriatic inflammation in the skin, notably *via* its ability to restrain the generation of inflammatory γδ T cells.

Finally, we tested whether other TLR ligands could also activate the Activin A-pSmad3C pathway. Macrophages treated for 6 h with the TLR9 ligand CpG, the TLR7/8 ligand R848 and the TLR2 ligand PamCysK all demonstrated induction of pSmad3C and *Inhba* expression (**Fig S11K and L**) demonstrating that the Activin A-Smad3 axis can be activated by several TLR ligand.

Discussion

In this study, we identified the Activin A-pSmad3C axis as a natural brake to inflammation put in place by macrophages to prevent their overt-activation. Importantly, this axis is activated by a variety of stimuli, including bacterial and viral ligands, as well as in the context of autoimmunity (**Fig S15**).

TGF-β has been demonstrated to be an important molecule to control inflammation in immune cells, including macrophages (12, 34-36). It is generally believed that pSmad3C is a marker of TGF-β signaling activation. Intriguingly, we observed that LPS, E protein and IMQ all induce pSmad3C in macrophages, which is independent of TGF-β signaling. Instead, Smad3 is phosphorylated by an autocrine Activin A-dependent loop, and therefore is dependent on the Activin A receptors (especially ACVR1B) in macrophages. This is of utmost importance since TGF-β and Activin A, besides their effects on Smad3, might have different functions and regulations, especially in diseases context. For example, it has been reported in CD4 T cells that Activin A drives the generation of pathogenic Th17 cells in the context of neuroinflammation but that TGF-β was unable to do it (37). In the context of sepsis and Covid-19, TGF-β appears to have a deleterious role (12, 38, 39). Moreover, during psoriasis, the overexpression of TGF-β in the epidermis leads to the development of psoriasis-like skin inflammation (40), overall demonstrating a divergent function between TGF-β and Activin A in these diseases. Our findings in this study have paved what we believe to be a new way to further understand how these two molecules differentially regulate innate immune responses and how to control them during diseases.

The role of Activin A in modulating macrophages functions is still unclear. Monocytes and other leukocytes have been shown to produce Activin A in response to LPS and in pediatric sepsis patients which was demonstrated to suppress the expression of inflammatory cytokines when added exogenously (41, 42). Some other reports however have suggested that Activin A has a pro-inflammatory effect on macrophages (43, 44). Notably, Jones et al reported that Activin A could be induced in the serum of mice after LPS treatment, and systemic treatment with Follistatin (to block Activin A) increased the survival of the mice. However, we clearly demonstrate here that genetic deletion of the Activin A receptor in macrophages is detrimental during sepsis. This possibly points out that Activin A could have a different effect on macrophages compared to other cells. It also suggests that Follistatin could have additional roles than only inhibiting Activin A. Moreover, the mechanisms by which Activin A production is regulated, as well as its downstream signaling and its detailed effect on macrophages phenotype and disease development remained poorly understood. Here, by using a combination of blocking antibody, Follistatin and most importantly macrophages conditional deletion of Activin A receptor *Acvr1b*, we studied in depth the role of the Activin A-Smad3 axis. We demonstrated that Activin A is naturally produced by macrophages, which is triggered by the activation of STAT5 in response to various inflammatory contexts. Activin A can therefore signal through Smad3 to pose a natural brake to innate inflammation. Mechanistically, we demonstrated that this axis is critical to regulate macrophages ATP metabolism which helps avoid having uncontrolled levels of inflammation in macrophages. Importantly, this axis protects mice against the development of overt-inflammation in models of sepsis, viral infection and psoriasis demonstrating a generalized mechanism, and suggesting that promoting

379 the Activin A-Smad3 pathway could provide a therapeutic strategy in these diseases. Indeed,
380 we also demonstrated that this axis was active in humans.

381 LPS regulates the inflammatory response by using a wide variety of mechanisms, including
382 metabolic reprogramming. It is now well appreciated that LPS promotes the induction of
383 glycolysis while it inhibits the mitochondrial metabolism (broken TCA cycle and decreased
384 OXPHOS) (22, 23, 45). Nevertheless, the mechanisms regulating these changes and how a
385 decreased mitochondrial metabolism regulates inflammation remains poorly understood. Here,
386 we have revealed that the Activin A-Smad3 axis supports the generation of mitochondria and
387 the maintenance of ATP production at homeostatic levels. In parallel, ATP is also converted into
388 adenosine by CD73 which can enforce the effect of Smad3 in regulating the expression of anti-
389 inflammatory molecules (such as *Arg1* and *Tgfbi*) in a CREB-dependent manner. This is in line
390 with the notion showing that CD73 and CREB can promote an anti-inflammatory phenotype in
391 macrophages (26, 27) and decipher a mechanism by which the LPS regulation of ATP
392 metabolism regulates inflammation. Although, our RNAseq data suggest that Smad3 regulates
393 mitochondrial biogenesis by transcriptional regulation of several genes involved in
394 mitochondrial function/biogenesis, future studies are needed to unravel the exact mechanisms
395 by which Smad3 regulates mitochondrial biogenesis as well as how and to what extent the
396 CD73-CREB axis controls the inflammatory response to inflammatory stimuli.

397 In summary, we have demonstrated that, in pro-inflammatory contexts, macrophages activate
398 pSmad3C in an Activin A-dependent, TGF-β-independent manner. This axis naturally protects
399 macrophages against overt-inflammatory responses and metabolic dysfunction in several
400 pathogenic contexts, including sepsis, Covid-19 and psoriasis. As the Activin A-Smad3 axis is

401 conserved in human macrophages, it may be targeted to harness new therapeutic strategies

402 during infections and autoimmunity.

Methods

Sex as a biological variable

Our study examined male and female animals, and similar findings are reported for both sexes. For sepsis experiments, because males are less susceptible to disease development, we only used female mice.

Mice

C57BL/6 mice were obtained from Jackson laboratory. *Smad3* KO mice and RI-Lyz2 cre mice were obtained as described previously (12, 46). *Acvr1b*-Lyz2 cre mice were generated by crossing *Acvr1b*$^{f/f}$ mice (generously gifted by Dr. Gloria H Su, Columbia university (20)) with Lyz2 cre mice. *Traf6* and *Stat5*-Lyz2 cre mice were generated by crossing *Traf6*$^{f/f}$ and *Stat5*$^{f/f}$ mice with Lyz2 cre mice (both obtained from Jackson laboratory). *Tlr4*, *Tlr7*, *MyD88* and *Trif* KO mice were obtained from Jackson laboratory. Mice were bred under specific pathogen-free conditions in the animal facility of National Institute of Dental and Craniofacial Research (NIDCR).

Human samples

For the generation of human macrophages, healthy donors were obtained from the NIH blood bank. Monocytes were isolated by elutriation (by the NIDCR CTRC core facility) and were differentiated for 7 days in presence of 10 % FBS (Fetal Bovine Serum) in RPMI (Thermofisher) supplemented with antibiotics (penicillin and streptomycin), Sodium pyruvate and glutamine but without fetal bovine serum (all from Gibco).

Cell culture

Mouse peritoneal macrophages and BMDMs were generated as described before (12). The cells were then cultured in RPMI containing antibiotics (Penicillin and Streptomycin), Sodium Pyruvate and Glutamine. The cells were treated with LPS (10 ng/mL, Sigma Aldrich), Activin A (100 ng/mL, R&D System), TGF-β (5 ng/mL, Peprotech), E protein (1 µg/mL, Abclonal), Imiquimod (1 µg/mL, InvivoGen), ATP (20 µM, Cayman Chemical), CpG ODN1826 (1 µM, InvivoGen), R848 (1 µg/ml, InvivoGen) or PamCysK (100 ng/ml, InvivoGen). Macrophages were pre-treated during 1 h before these treatments with Follistatin (0.5 µg/mL, Biolegend), CHX (5 µM, Cayman Chemical), anti-TGF-β antibody (50 µg/mL, Bioxcell), anti-Activin A antibody (2 µg/mL, R&D Systems), Smad3 inhibitor (SIS3, 2µM, Cayman Chemical), TAK1 inhibitor (5 nM, Sigma Aldrich), MEK inhibitor (10 µM, Cayman Chemical), ERK inhibitor (1 µM, Cayman Chemical), STAT5 inhibitor (100 µM, Cayman Chemical), CD73 inhibitor (10 µM, Cayman Chemical) and CREB inhibitor (1 µM, Cayman Chemical).

Western blotting

Tissue lysates from macrophages were prepared in NP-40 lysis buffer (NP-40 1%, Tris pH 7.5 20 mM, NaCl 150 mM, EDTA 2.5 mM, NaF 10 mM NaPPi (Sodium Pyruphosphate) 10 mM, PMSF 10mM, NaDeoxycholate 0.25%, Na3VO4 1mM and proteinase inhibitors: Aprotinin, Leupeptin, Pepstatin A, 5 µg/ml each (all from Sigma-Aldrich except PMSF from Fluka Biochemika). Protein samples were separated on 10% Tris-Glycine gels (Thermo Fisher Scientific) and transferred to PVDF membranes (Thermo Fisher Scientific). The membranes were soaked in blocking buffer (Milk 5%, Biorad) for 1 hour at room temperature and subsequently incubated with the

appropriate primary antibodies overnight at 4˚C. Next day, the membranes were washed and incubated for 1 hour at room temperature with HRP-conjugated secondary antibodies (Cell signaling technology). Immunoreactivity was detected using ECL and acquired with an Amersham Imager 600 (General Electric) followed by stripping the membranes with Restore Plus Western blot stripping buffer (Thermo fisher) and incubated with GAPDH antibody (Sigma-Aldrich) as a control. Data were quantified using image J (NIH).

RT-qPCR

RNA from cells was extracted using RNeasy Plus Micro kit (Qiagen) following the manufacturer recommendations. cDNA was synthesized using a High Capacity cDNA Reverse Transcription Kit (Thermo Fisher). qPCR was performed using TaqMan Master Mix (Thermo Fisher). The primers used are listed in Supplementary Table 1. Total transcripts values were normalized using mouse or human *Hprt*. Results were calculated using the comparative ΔΔCt method (47). Results are shown as fold change compared to control.

ELISA

The levels of TNF-α, IL-6 (Biolegend), Activin A (R&D Systems) and ATP (Cayman Chemical) were measured in the supernatant and the serum by ELISA (Enzyme-linked immunosorbent assay) according to the manufacturer recommendations.

Detection of TGF-β signaling with the MFB-F11 reporter cells

This experiment was performed as previously described (18, 19). Briefly, MFB-F11 cells (fibroblast cell line isolated from mouse *Tgfb1*$^{-/-}$ embryos (MFB) stably transfected with the SBE-

SEAP reporter) were seeded at a density of 30,000 cells per well in 96-well flat-bottom tissue culture plates. After an overnight incubation, the cells were washed with PBS followed by the addition of 50 µl of serum-free Dulbecco's modified Eagle's medium (DMEM) supplemented with penicillin and streptomycin (DMEM/P/S) and 1x B27 supplement (test media) for 2 hours. The individual samples, which included treatments with recombinant TGF-β1 in the presence of the neutralizing anti-TGF-β Ab 1D11 or an isotype control, were then prepared in a final volume of 50 µl of test media and added to the cells for a final volume of 100 µl. The cells were incubated for 18-24 hours, after which the supernatants were collected and stored at -20°C. The induction of secreted alkaline phosphatase (SEAP) was measured in the collected supernatants with the Great EscAPe™ SEAP Chemiluminescence Kit (Promega) as previously described(18, 19).

CHIP assay

The Ideal CHIP-qPCR kit (Diagenode) was used according to the manufacturer's instructions to perform CHIP experiments. 4 million cultured macrophages with or without LPS during 2 h were used per condition. An equal amount of processed chromatin was used as an input control or was incubated with an anti-c-STAT5 antibody (Abcam) or its isotype-matched control antibody (rabbit IgG, Abcam). Immunoprecipitated DNA and total input DNA were analyzed with a SYBR Green Supermix kit. Results after immunoprecipitation were normalized with the input and IgG. The sequence of primers is provided in Supplementary Table 2.

FACS and immunofluorescence staining

Cells were stained with the Zombie Yellow Fixable Viability Kit (Biolegend) for 10 min at 4 ˚C followed by surface staining with anti-mouse antibodies (CD45 for immune cells, CD11b, CD64, for macrophages, TCRβ, TCRγδ for γδT cells) during 20 min at 4°C in presence of FCγ receptors blocking antibodies. Intracellular staining was performed using the Perm/Wash buffer set (BD Biosciences) during 20 min at 4°C followed by staining with anti-mouse antibodies (IFN-γ, IL-17A, IL-22, IL-6 and TNF-α). For cytokines staining, cells were stimulated during 4 h at 37°C with PMA (5 ng/mL), Ionomycin (1 ug/mL) and Golgi-Plug (1/1000 dilution, BD Biosciences). Cells were analyzed on the BD LSRFortessa analyzer.

For analysis of pSmad2/3C by flow cytometry, peritoneal cells were fixed using 4 % of paraformaldehyde for 20 min at 37 ˚C followed by a PBS wash. Cells were then permeabilized with 90 % methanol overnight at -20 ˚C, followed by 2 washes with PBS. Cells were then stained with pSmad2/3C antibody (Cell Signaling Technology) for 45 min at 4 ˚C followed by a wash and staining with an anti-rabbit Alexa Fluor 488 secondary antibody (Thermo Fisher) for 45 min at 4 ˚C. with anti-Ly6G, F4/80, CD11c, CD3 and CD19 to identify neutrophils, macrophages, dendritic cells, T cells and B cells.

For mitochondrial staining, macrophages were stained at 37 ˚C with TMRM (50 nM for 30 min), mitoSOx red (5 µM for 10 min) and mitotracker green (100 nM for 30 min) in RPMI. For immunofluorescence, cells were further permeabilized with methanol for 15 min at 4 ˚C, washed and stained with DAPI for 5 minutes (1 ug/mL, ThermoFisher, 62247) before mounting on slides and acquired with a Nikon A1R+ MP. Data were quantified using image J.

RNA sequencing

Total RNA was reverse transcribed by Superscript IV (Invitrogen, Carlsbad, CA) using template switching oligo and oligo dT primers followed by amplification of the second strand cDNA with LongAmp Taq polymerase (New England Biolabs, Ipswich, MA). Libraries were prepared using the Nextera XT method (Illumina, San Diego, CA) kit, individually barcoded, and sequenced on a NextSeq 2000 instrument (Illumina) using 100 x 100 paired-end mode. The fastq files were aligned to the mouse genome (GRCm38) using vM11 annotation and gene counts generated using STAR (v2.7.3a). An expression matrix of raw gene counts was filtered to remove low counts genes (defined as those with less than 5 reads in at least one sample). The filtered expression matrix was analyzed in DESeq2 to find differentially expressed genes (48).

Sepsis models

Mice were injected with 15 mg/kg of LPS from *E.coli* (Sigma-Aldrich). Survival rates were monitored for 96 h and serum was extracted, 3 h after LPS injection, from the blood, following by a centrifugation of 20 min at room temperature. Mice defined as "WT" are littermates *Acvr1b*$^{+/+}$Lyz2 cre + (as opposed to *Acvr1b*-Lyz2 cre mice which are *Acvr1b*$^{fl/fl}$Lyz2 cre +).

For the CLP-induced sepsis model(12), mice were subjected to a midline laparotomy followed by a ligation of ∼50 % of the cecum to induce sepsis. A single through-and-through puncture with a 19 G needle was then made distal to the ligature. Survival rates were monitored for 7 days and serum was harvested at 18 h.

Psoriasis model

62.5 mg of imiquimod (or Vaseline as a control) was applied onto the back of shaved mice for 6 consecutive days. Tissues were homogenized using beads 2.0 mm zirconia beads (Biospec) and

Trizol reagent according to the manufacturer instructions (Qiagen). For Western blotting, tissue was homogenized using T-PER buffer (Thermo Fisher) supplemented with protease inhibitor (cOmplete Mini, Sigma-Aldrich) and phosphatase inhibitor (PhosSTOP, Roche). Cells were extracted by cutting and incubating the skin at 37 ˚C in 500 µg/mL of Liberase DH (Roche) dissolved in HBSS during 1 h. After incubation, the skin was smashed through a 70 µm strainer and filtered a second time before FACS staining as described above. For the macrophages transfer experiments, 0.5 million thioglycolate-elicited macrophages, isolated from WT or *Smad3* KO mice, were injected intradermally (in 2 sites) in CD45.1 mice right before the first imiquimod application. For the blocking antibodies experiment, anti TNF-α, IL-6, IL-1β and IL-23A antibodies (or IgG control; 100 µg of each antibody or 400 µg of IgG control) were injected i.p 24 h before the first imiquimod application and again at D4. The list of all the antibodies used in this study is provided in Supplementary Table 3. For histology, organs were fixed in formalin 10% (Thermo Fisher Scientific), paraffin-embedded, and cut in 4-µm sections. Tissues were stained with hematoxylin and eosin, and acquisition was performed using a Nanozoomer S60 (Hamamatsu). For the bone marrow chimeras (BM chimeras), CD45.1 mice were lethally irradiated (950 rads) before injection of 5 millions cells from CD45.2 WT or *Smad3* KO BM 5h after irradiation. Trimethoprim-Sulfamethoxazole was given for 2 weeks and autoclaved cages were used to house the animals. Four weeks after reconstitution, IMQ was applied for 6 days as described above.

Statistical analysis

Statistical analyses were performed using GraphPad Prism 8 software. Data are presented as mean ± SEM. Statistical significance ($P < 0.05$) was determined by unpaired *t* test (two-tailed,

two groups), one-way analysis of variance (ANOVA) (more than two groups), or log-rank (Mantel-Cox) test (survival curve). Identified outliers were excluded. Statistical analysis was performed in all the required experiments. All experiments were performed at least twice independently.

Study approval

Animal studies were performed according to National Institutes of Health (NIH) guidelines and approved by the NIDCR Animal Care and Use Committee (ACUC).

Data availability

All the graphics supporting data are provided in an XLS file document. RNAseq data have been deposited on the GEO database (GSE284154).

Author Contributions

T. G. conceived the research, designed and performed the experiments, analyzed data and drafted the manuscript. Y.L, W.J, N.L, L.P, W.C, J.W and G.D performed and analyzed experiments. D.M and R.M analyzed the RNAseq data. G.S provided the *Acvr1b* flox mice. W.J.C conceived and supervised the research, designed the experiments and wrote the manuscript.

Acknowledgements

This research was supported by the Intramural Research Programs, National Institutes of Health (NIDCR and NIDCD). We thank the Genomics and Biotechnology Core for sequencing (ZIC DC000086 to the GCBC) and the Combined Technical Research Core and Veterinary Resources Core at NIDCR for service and technical assistance. This work was prepared while Dr. Gloria Su was employed at Columbia University Irving Medical Center. The opinions expressed in this article are Dr. Su's own and do not reflect the view of the National Institutes of Health, the Department of Health and Human Services, or the United States government. We thank Dr. Ana Costa da Silva and Dr. Mladen Mitrovic for their assistance with experiments and analysis. This work utilized the computational resources of the NIH HPC Biowulf cluster. (http://hpc.nih.gov). BioRender was used to generate figure S7J and S15.

Declaration of Interests

The authors declare no competing interests.

Legend

Figure 1. LPS activates Smad3 in a TGF-β independent manner (**A**) Abundance of the indicated proteins in macrophages treated with 10 ng/mL of LPS for the indicated time points. (**B**) Abundance of the indicated proteins in macrophages pre-treated with cycloheximide for 1 h followed by LPS stimulation for 6 h. (**C**) Abundance of the indicated proteins in macrophages pre-treated with an anti-TGF-β blocking antibody for 1 h followed by LPS or TGF-β (5 ng/mL) stimulation for 6 h. (**D**) Abundance of the indicated proteins in macrophages isolated from WT or RI-Lyz2 cre mice and stimulated by LPS or TGF-β for 6 h. (**E**) Abundance of the indicated proteins in peritoneal cells of mice injected i.p with LPS and harvested 6 h after injection. Each band represents a mouse. (**F**) Flow cytometry analysis of phosphorylated Smad2/3 (pSmad2/3) levels in peritoneal cells from mice injected i.p with LPS and harvested 6 h after injection. MFI= Mean Fluorescence Intensity. M= Macrophages, N= Neutrophils, DC= Dendritic Cells, B= B cells, T= T cells. (n=9) (**G**) Flow cytometry analysis of pSmad2/3 levels in macrophages from WT or RI-Lyz2 cre mice injected i.p with LPS and harvested 6 h after injection. Red= Isotype control, Orange= WT, Blue= WT LPS, Green= RI-Lyz2 cre LPS. (**H**) Abundance of the indicated proteins in peritoneal cells of mice subjected to CLP-surgery (or Sham-surgery) and harvested 6 h after injection. Each band represents a mouse. (**I**) Flow cytometry analysis of pSmad2/3 levels in macrophages from WT or RI-Lyz2 cre mice subjected to CLP-surgery (or Sham-surgery) and harvested 6 h after injection. Red= Isotype control, Green= WT, Blue= WT LPS, Orange= RI-Lyz2 cre LPS. Representative or pooled of at least 2 independent experiments. **P<0.01, ***P<0.005, ****P<0.001 by one-way ANOVA.

Figure 2. LPS phosphorylates Smad3 in an Activin A dependent manner (**A**) RT-qPCR analysis of the indicated genes in macrophages stimulated by LPS for 2, 4 or 6 h. (n=4-6) (**B**) Activin A levels (measured by ELISA) in the supernatant of macrophages stimulated by LPS for 2, 4 or 6 h. (**C**) Abundance of the indicated proteins in macrophages isolated from WT or *Acvr1b*-Lyz2 cre mice (KO) and stimulated by LPS for 6 h. (**D**) RT-qPCR analysis of *INHBA* expression in human macrophages stimulated by LPS for 6 h. (n=4) (**E**) Abundance of the indicated proteins in human macrophages pre-treated with Follistatin, an anti-Activin A or an anti-TGF-β blocking antibody for 1 h followed by LPS stimulation for 6 h. (**F**) Activin A levels (measured by ELISA) in the serum of WT mice injected i.p with LPS and harvested 6 h after injection. (n=10) (**G**) Activin A levels (measured by ELISA) in the serum of WT mice subjected to CLP-surgery (or Sham-surgery) and harvested 6 h after surgery. (n=6) (**H**) Flow cytometry analysis of pSmad2/3 levels in macrophages from WT or *Acvr1b*-Lyz2 cre mice injected i.p with LPS and harvested 6 h after surgery. (**I**) Flow cytometry analysis of pSmad2/3 levels in macrophages from WT or *Acvr1b*-Lyz2 cre mice subjected to CLP-surgery (or Sham-surgery) and harvested 6 h after injection. (**J**) RT-qPCR analysis of the indicated genes in macrophages from WT or *Acvr1b*-Lyz2 cre mice stimulated or not by LPS for 24 h. (n=4-6) (**K**) RT-qPCR analysis of the indicated genes in macrophages from WT or *Smad3* KO mice stimulated or not by LPS for 24 h. (n=4) (**L**) RT-qPCR analysis of *IL6* expression in human macrophages pre-treated with Follistatin or an anti-Activin A blocking antibody for 1 h followed by LPS stimulation for 24 h. (n=4) (**M**) RT-qPCR analysis of *IL6* expression in human macrophages pre-treated with a Smad3 inhibitor (SMAD3i) for 1 h followed by LPS stimulation for 24 h. (n=4) (**N**) RT-qPCR analysis of the indicated genes in macrophages from WT (upper panel) or *Smad3* KO (lower panel) mice stimulated by LPS for 24

h in presence or absence of Activin A. (n=6) Representative or pooled from at least 2 independent experiments. *P<0.05, **P<0.01, ***P<0.005, ****P<0.001 by Student's T test (A, B, D, F, G and N) or one-way ANOVA (H-M).

Figure 3. LPS induces the Activin A-Smad3 axis through a TLR4-Myd88-MAPK-STAT5 pathway

(**A**) RT-qPCR analysis of *Inhba* expression in macrophages from WT or *TLR4* KO mice stimulated by LPS for 2 h. (n=6) (**B**) RT-qPCR analysis of *Inhba* expression in macrophages from WT or MyD88 KO mice stimulated by LPS for 2 h. (n=4) (**C**) Abundance of the indicated proteins in macrophages isolated from WT, *MyD88* or *TLR4* KO mice and stimulated by LPS for 6 h. (**D**) RT-qPCR analysis of *Inhba* expression in macrophages from WT or *Traf6*-Lyz2 cre mice stimulated by LPS for 2 h. (n=6) (**E**) Abundance of the indicated proteins in macrophages isolated from WT or *Traf6*-Lyz2 cre mice and stimulated by LPS for 6 h. (**F**) RT-qPCR analysis of *Inhba* expression in macrophages pre-treated with a TAK1 inhibitor for 1 h followed by LPS stimulation for 2 h. (n=6) (**G**) Abundance of the indicated proteins in macrophages pre-treated with a TAK1 inhibitor for 1 h followed by LPS stimulation for 6 h. (**H**) RT-qPCR analysis of *Inhba* expression in macrophages pre-treated with MEK and ERK inhibitors for 1 h followed by LPS stimulation for 2 h. (n=6) (**I**) Abundance of the indicated proteins in macrophages pre-treated with MEK and ERK inhibitors for 1 h followed by LPS stimulation for 6 h. (**J**) Abundance of the indicated proteins in macrophages treated with LPS for the indicated times. (**K**) CHIP-coupled real-time PCR analysis of STAT5 enrichment in various sequences of the promoter region of *Inhba* gene in macrophages treated with LPS for 2 h. (n=6) (**L**) RT-qPCR analysis of *Inhba* expression in macrophages pre-treated with a STAT5 inhibitor for 1 h followed by LPS stimulation for 2 h. (n=6) (**M**) Abundance of the indicated proteins in macrophages pre-treated with a STAT5

inhibitor for 1 h followed by LPS stimulation for 6 h. (**N**) RT-qPCR analysis of *Inhba* expression in macrophages from WT or *Stat5*-Lyz2 cre mice stimulated by LPS for 2 h. (n=6) (**O**) Abundance of the indicated proteins in macrophages isolated from WT or *Stat5*-Lyz2 cre mice and stimulated by LPS for 6 h. Representative of at least 2 independent experiments. *P<0.05, **P<0.01, ***P<0.005, ****P<0.001 by one-way ANOVA.

Figure 4. The Activin A-Smad3 pathway supports ATP metabolism during inflammation (**A**) Heatmap representing significantly down-regulated genes in macrophages from *Smad3* KO mice (compared to WT macrophages) stimulated with LPS for 24 h. Mitotracker staining in macrophages stimulated with LPS for 24 h and isolated from *Smad3* KO mice (**B**) or *Acvr1b*-Lyz2 cre mice (**C**). ATP production (intracellular) in macrophages stimulated with LPS for 24 h and isolated from *Smad3* KO mice (**D**) (n=6) or *Acvr1b*-Lyz2 cre mice (**E**). RT-qPCR analysis of *Arg1* and *Tgfbi* expression in macrophages stimulated with LPS for 24 h in combination (or not) with 20 µM of ATP and isolated from *Smad3* KO mice (**F**) or *Acvr1b*-Lyz2cre mice (**G**). (**H**) RT-qPCR analysis of *Nt5e* expression (encoding CD73) in macrophages stimulated with LPS for 24 h and isolated from *Smad3* KO or *Acvr1b*-Lyz2 cre mice. RT-qPCR analysis of *Tgfbi* and *Arg1* expression in macrophages stimulated with LPS for 24 h in combination (or not) with ATP and a CD73 inhibitor or a CREB inhibitor and isolated from *Smad3* KO mice (**I**) or *Acvr1b*-Lyz2 cre mice (**J**). (F-J, n=4). Representative of at least 2 independent experiments. *P<0.05, **P<0.01, ***P<0.005, ****P<0.001 by student's T test (B-G) one-way ANOVA (H-J).

Figure 5. Activin A signaling in macrophages controls inflammation and survival during sepsis (**A**) Survival of WT or *Acvr1b*-Lyz2 cre mice injected intraperitoneally with LPS. (n=8-13) (**B**) TNF-α and IL-6 levels in serum of WT or *Acvr1b*-Lyz 2cre mice injected intraperitoneally or not with

LPS for 3 h. (n=6-13) (**C**) Survival of WT or *Acvr1b*-Lyz2 cre mice subjected to CLP-surgery. (n=7-11) (**D**) TNF-α and IL-6 levels in serum of WT or *Acvr1b*-Lyz2 cre mice subjected to CLP-surgery. (n=8-12). Pooled from at least 2 independent experiments. *P<0.05 by log-rank (Mantel-Cox test, A and C) and student's T test (B and D).

Figure 6. The Activin A-Smad3 axis regulates inflammation during psoriasis (**A**) RT-qPCR analysis of *Inhba* expression in macrophages pre-treated for 1 h with the indicated inhibitors and stimulated with Imiquimod (IMQ) for 2 h. (n=4-6) (**B**) Abundance of the indicated proteins in macrophages isolated from WT or *Acvr1b*-Lyz2 cre mice (KO) and stimulated with IMQ for 6 h. (**C**) RT-qPCR analysis of *INHBA* expression in human monocytes stimulated with IMQ for 2 h. (n=4) (**D**) Abundance of the indicated proteins in human monocytes pre-treated with Follistatin, an anti-Activin A or an anti-TGF-β blocking antibody for 1 h followed by IMQ stimulation for 6 h. (**E**) RT-qPCR analysis of the indicated genes in macrophages from WT or *Acvr1b*-Lyz2 cre mice stimulated or not with IMQ for 24 h. (n=4) (**F**) RT-qPCR analysis of the indicated genes in macrophages from WT or *Smad3* KO mice stimulated or not with IMQ for 24 h. (n=4) (**G**) RT-qPCR analysis of *Inhba* expression in the skin of WT mice treated with an IMQ topical application for 6 h. (n=10) (**H**) Abundance of the indicated proteins in the skin of WT mice treated with an IMQ topical application for 6 h. Each band represents a mouse. Macrophages from WT or *Smad3* KO macrophages were transferred intradermally in the skin of CD45.1 WT mice followed by IMQ topical application for 6 consecutive days. Mice were then harvested and analyzed. (**I**) Skin thickness. (n=15) (**J**) TCRγδ cytokines production in the skin. (n=15) WT or *Acvr1b*-Lyz2 cre were treated with IMQ topical application for 6 consecutive days, then harvested and analyzed. (**K**) Skin thickness. (**L**) Macrophages frequency in the skin. (**M**)

689 Production of cytokines by macrophages. (**N**) TCRγδ cytokines production in the skin. (K-N, n=8-

690 9) Representative or pooled of at least 2 independent experiments. *P<0.05, **P<0.01,

691 ***P<0.005, ****P<0.001 by student's T test (C, G-N) or one-way ANOVA (A, E, F and O).

692

1. Murray PJ, and Wynn TA. Protective and pathogenic functions of macrophage subsets. *Nat Rev Immunol.* 2011;11(11):723-37.
2. Park MD, Silvin A, Ginhoux F, and Merad M. Macrophages in health and disease. *Cell.* 2022;185(23):4259-79.
3. Watanabe S, Alexander M, Misharin AV, and Budinger GRS. The role of macrophages in the resolution of inflammation. *J Clin Invest.* 2019;129(7):2619-28.
4. Martin-Rodriguez O, Gauthier T, Bonnefoy F, Couturier M, Daoui A, Chague C, et al. Pro-Resolving Factors Released by Macrophages After Efferocytosis Promote Mucosal Wound Healing in Inflammatory Bowel Disease. *Front Immunol.* 2021;12:754475.
5. Wynn TA, and Vannella KM. Macrophages in Tissue Repair, Regeneration, and Fibrosis. *Immunity.* 2016;44(3):450-62.
6. Gauthier T, Martin-Rodriguez O, Chague C, Daoui A, Ceroi A, Varin A, et al. Amelioration of experimental autoimmune encephalomyelitis by in vivo reprogramming of macrophages using pro-resolving factors. *J Neuroinflammation.* 2023;20(1):307.
7. Bonnefoy F, Gauthier T, Vallion R, Martin-Rodriguez O, Missey A, Daoui A, et al. Factors Produced by Macrophages Eliminating Apoptotic Cells Demonstrate Pro-Resolutive Properties and Terminate Ongoing Inflammation. *Front Immunol.* 2018;9:2586.
8. Fadok VA, Bratton DL, Konowal A, Freed PW, Westcott JY, and Henson PM. Macrophages that have ingested apoptotic cells in vitro inhibit proinflammatory cytokine production through autocrine/paracrine mechanisms involving TGF-beta, PGE2, and PAF. *J Clin Invest.* 1998;101(4):890-8.
9. Batlle E, and Massague J. Transforming Growth Factor-beta Signaling in Immunity and Cancer. *Immunity.* 2019;50(4):924-40.
10. Gauthier T, and Chen W. IFN-gamma and TGF-beta, Crucial Players in Immune Responses: A Tribute to Howard Young. *J Interferon Cytokine Res.* 2022;42(12):643-54.
11. Chen W, and Ten Dijke P. Immunoregulation by members of the TGFbeta superfamily. *Nat Rev Immunol.* 2016;16(12):723-40.
12. Gauthier T, Yao C, Dowdy T, Jin W, Lim YJ, Patino LC, et al. TGF-beta uncouples glycolysis and inflammation in macrophages and controls survival during sepsis. *Sci Signal.* 2023;16(797):eade0385.
13. Chen B, Huang S, Su Y, Wu YJ, Hanna A, Brickshawana A, et al. Macrophage Smad3 Protects the Infarcted Heart, Stimulating Phagocytosis and Regulating Inflammation. *Circ Res.* 2019;125(1):55-70.
14. Afroz R, Kumarapperuma H, Nguyen QVN, Mohamed R, Little PJ, and Kamato D. Lipopolysaccharide acting via toll-like receptor 4 transactivates the TGF-beta receptor in vascular smooth muscle cells. *Cell Mol Life Sci.* 2022;79(2):121.
15. Konkel JE, Maruyama T, Carpenter AC, Xiong Y, Zamarron BF, Hall BE, et al. Control of the development of CD8alphaalpha+ intestinal intraepithelial lymphocytes by TGF-beta. *Nat Immunol.* 2011;12(4):312-9.
16. Martinez GJ, Zhang Z, Chung Y, Reynolds JM, Lin X, Jetten AM, et al. Smad3 differentially regulates the induction of regulatory and inflammatory T cell differentiation. *J Biol Chem.* 2009;284(51):35283-6.

17. Park SA, Lim YJ, Ku WL, Zhang D, Cui K, Tang LY, et al. Opposing functions of circadian protein DBP and atypical E2F family E2F8 in anti-tumor Th9 cell differentiation. *Nat Commun.* 2022;13(1):6069.
18. Tesseur I, Zou K, Berber E, Zhang H, and Wyss-Coray T. Highly sensitive and specific bioassay for measuring bioactive TGF-beta. *BMC Cell Biol.* 2006;7:15.
19. Blois SM, Sulkowski G, Tirado-Gonzalez I, Warren J, Freitag N, Klapp BF, et al. Pregnancy-specific glycoprotein 1 (PSG1) activates TGF-beta and prevents dextran sodium sulfate (DSS)-induced colitis in mice. *Mucosal Immunol.* 2014;7(2):348-58.
20. Qiu W, Li X, Tang H, Huang AS, Panteleyev AA, Owens DM, et al. Conditional activin receptor type 1B (Acvr1b) knockout mice reveal hair loss abnormality. *J Invest Dermatol.* 2011;131(5):1067-76.
21. Watts C. Location, location, location: identifying the neighborhoods of LPS signaling. *Nat Immunol.* 2008;9(4):343-5.
22. Gauthier T, and Chen W. Modulation of Macrophage Immunometabolism: A New Approach to Fight Infections. *Front Immunol.* 2022;13:780839.
23. Wculek SK, Dunphy G, Heras-Murillo I, Mastrangelo A, and Sancho D. Metabolism of tissue macrophages in homeostasis and pathology. *Cell Mol Immunol.* 2022;19(3):384-408.
24. Basso PJ, Gauthier T, Palomares F, Lopez-Enriquez S, and Tsai S. Editorial: Immunometabolism: bridging the gap between immunology and nutrition. *Front Nutr.* 2024;11:1436894.
25. Dunn J, and Grider MH. *StatPearls*. Treasure Island (FL); 2023.
26. Antonioli L, Pacher P, Vizi ES, and Hasko G. CD39 and CD73 in immunity and inflammation. *Trends Mol Med.* 2013;19(6):355-67.
27. Nemeth ZH, Leibovich SJ, Deitch EA, Sperlagh B, Virag L, Vizi ES, et al. Adenosine stimulates CREB activation in macrophages via a p38 MAPK-mediated mechanism. *Biochem Biophys Res Commun.* 2003;312(4):883-8.
28. Lv KY, Zhong QS, Liu XF, Zhu SH, Xiao SC, Wang GY, et al. Deficiency of Smad3 results in enhanced inducible nitric oxide synthase-mediated hypotension in lipopolysaccharide-induced endotoxemia. *J Surg Res.* 2014;187(2):640-5.
29. Reyes M, Filbin MR, Bhattacharyya RP, Billman K, Eisenhaure T, Hung DT, et al. An immune-cell signature of bacterial sepsis. *Nat Med.* 2020;26(3):333-40.
30. Olwal CO, Nganyewo NN, Tapela K, Djomkam Zune AL, Owoicho O, Bediako Y, et al. Parallels in Sepsis and COVID-19 Conditions: Implications for Managing Severe COVID-19. *Front Immunol.* 2021;12:602848.
31. Merad M, and Martin JC. Pathological inflammation in patients with COVID-19: a key role for monocytes and macrophages. *Nat Rev Immunol.* 2020;20(6):355-62.
32. Zheng M, Karki R, Williams EP, Yang D, Fitzpatrick E, Vogel P, et al. TLR2 senses the SARS-CoV-2 envelope protein to produce inflammatory cytokines. *Nat Immunol.* 2021;22(7):829-38.
33. Zanvit P, Konkel JE, Jiao X, Kasagi S, Zhang D, Wu R, et al. Antibiotics in neonatal life increase murine susceptibility to experimental psoriasis. *Nat Commun.* 2015;6:8424.

34. Chen W, Jin W, Hardegen N, Lei KJ, Li L, Marinos N, et al. Conversion of peripheral CD4+CD25- naive T cells to CD4+CD25+ regulatory T cells by TGF-beta induction of transcription factor Foxp3. *J Exp Med.* 2003;198(12):1875-86.
35. Zhang D, Jin W, Wu R, Li J, Park SA, Tu E, et al. High Glucose Intake Exacerbates Autoimmunity through Reactive-Oxygen-Species-Mediated TGF-beta Cytokine Activation. *Immunity.* 2019;51(4):671-81 e5.
36. Gong D, Shi W, Yi SJ, Chen H, Groffen J, and Heisterkamp N. TGFbeta signaling plays a critical role in promoting alternative macrophage activation. *BMC Immunol.* 2012;13:31.
37. Wu B, Zhang S, Guo Z, Bi Y, Zhou M, Li P, et al. The TGF-beta superfamily cytokine Activin-A is induced during autoimmune neuroinflammation and drives pathogenic Th17 cell differentiation. *Immunity.* 2021;54(2):308-23 e6.
38. Ferreira-Gomes M, Kruglov A, Durek P, Heinrich F, Tizian C, Heinz GA, et al. SARS-CoV-2 in severe COVID-19 induces a TGF-beta-dominated chronic immune response that does not target itself. *Nat Commun.* 2021;12(1):1961.
39. Witkowski M, Tizian C, Ferreira-Gomes M, Niemeyer D, Jones TC, Heinrich F, et al. Untimely TGFbeta responses in COVID-19 limit antiviral functions of NK cells. *Nature.* 2021;600(7888):295-301.
40. Li AG, Wang D, Feng XH, and Wang XJ. Latent TGFbeta1 overexpression in keratinocytes results in a severe psoriasis-like skin disorder. *EMBO J.* 2004;23(8):1770-81.
41. Shao L, Frigon NL, Jr., Sehy DW, Yu AL, Lofgren J, Schwall R, et al. Regulation of production of activin A in human marrow stromal cells and monocytes. *Exp Hematol.* 1992;20(10):1235-42.
42. Petrakou E, Fotopoulos S, Anagnostakou M, Anatolitou F, Samitas K, Semitekolou M, et al. Activin-A exerts a crucial anti-inflammatory role in neonatal infections. *Pediatr Res.* 2013;74(6):675-81.
43. Jones KL, Mansell A, Patella S, Scott BJ, Hedger MP, de Kretser DM, et al. Activin A is a critical component of the inflammatory response, and its binding protein, follistatin, reduces mortality in endotoxemia. *Proc Natl Acad Sci U S A.* 2007;104(41):16239-44.
44. Sierra-Filardi E, Puig-Kroger A, Blanco FJ, Nieto C, Bragado R, Palomero MI, et al. Activin A skews macrophage polarization by promoting a proinflammatory phenotype and inhibiting the acquisition of anti-inflammatory macrophage markers. *Blood.* 2011;117(19):5092-101.
45. Jha AK, Huang SC, Sergushichev A, Lampropoulou V, Ivanova Y, Loginicheva E, et al. Network integration of parallel metabolic and transcriptional data reveals metabolic modules that regulate macrophage polarization. *Immunity.* 2015;42(3):419-30.
46. Han J, Liu N, Jin W, Zanvit P, Zhang D, Xu J, et al. TGF-beta controls development of TCRgammadelta(+)CD8alphaalpha(+) intestinal intraepithelial lymphocytes. *Cell Discov.* 2023;9(1):52.
47. Ceroi A, Delettre FA, Marotel C, Gauthier T, Asgarova A, Biichle S, et al. The anti-inflammatory effects of platelet-derived microparticles in human plasmacytoid dendritic cells involve liver X receptor activation. *Haematologica.* 2016;101(3):e72-6.
48. Love MI, Huber W, and Anders S. Moderated estimation of fold change and dispersion for RNA-seq data with DESeq2. *Genome Biol.* 2014;15(12):550.

β

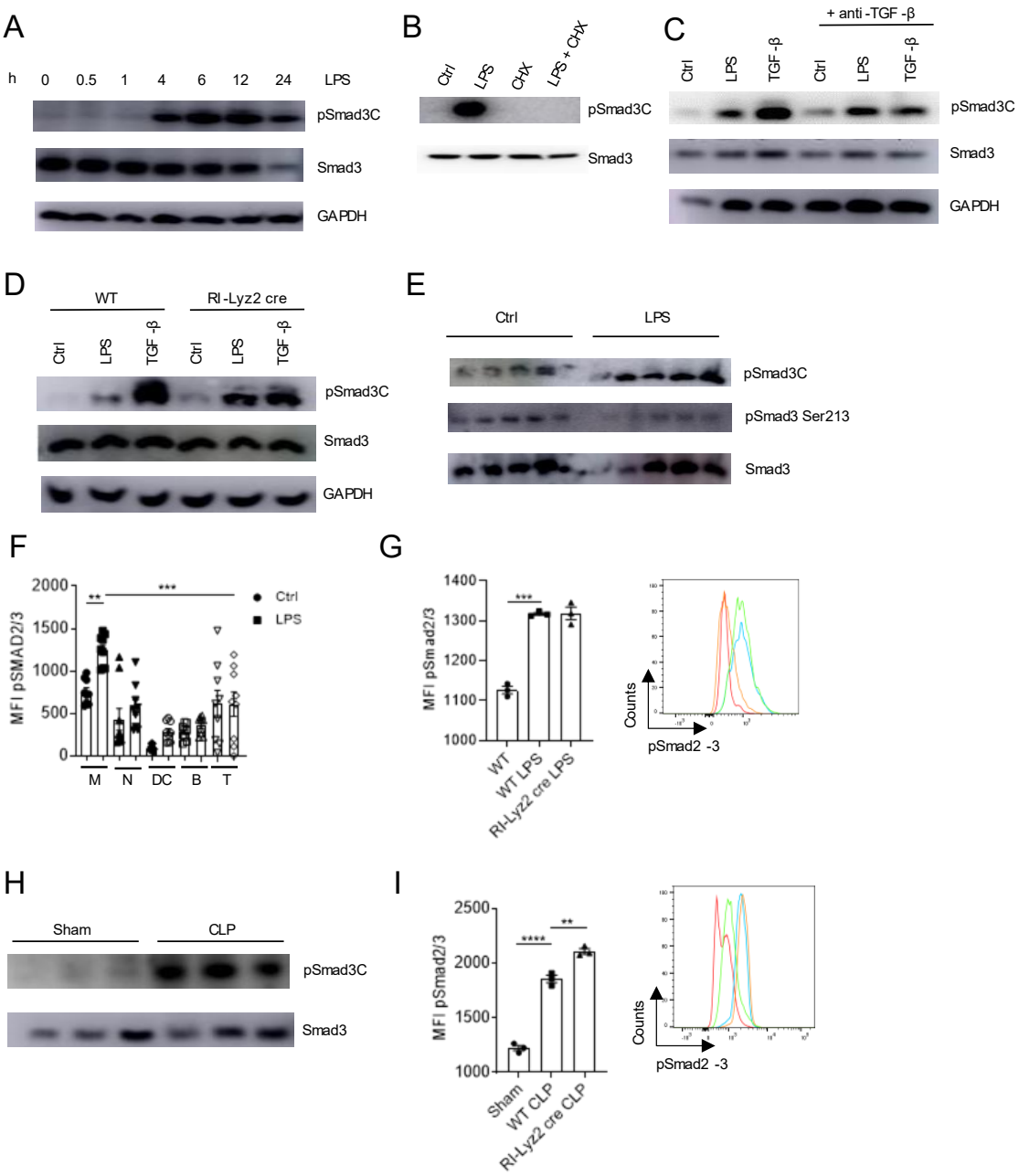
A
h 0 0.5 1 4 6 12 24 LPS
pSmad3C
Smad3
GAPDH
B
Ctrl LPS CHX LPS + CHX
pSmad3C
Smad3
C
+ anti -TGF -β
Ctrl LPS TGF -β Ctrl LPS TGF -β
pSmad3C
Smad3
GAPDH
D
WT
RI -Lyz2 cre
Ctrl LPS TGF -β Ctrl LPS TGF -β
pSmad3C
Smad3
GAPDH
E
Ctrl
LPS
pSmad3C
pSmad3 Ser213
Smad3
F
MFI pSMAD2/3
Ctrl
LPS
M N DC B T
G
MFI pSmad2/3
WT
WT LPS
RI-Lyz2 cre LPS
Counts
pSmad2 -3
H
Sham
CLP
pSmad3C
Smad3
I
MFI pSmad2/3
Sham
WT CLP
RI-Lyz2 cre CLP
Counts
pSmad2 -3

951

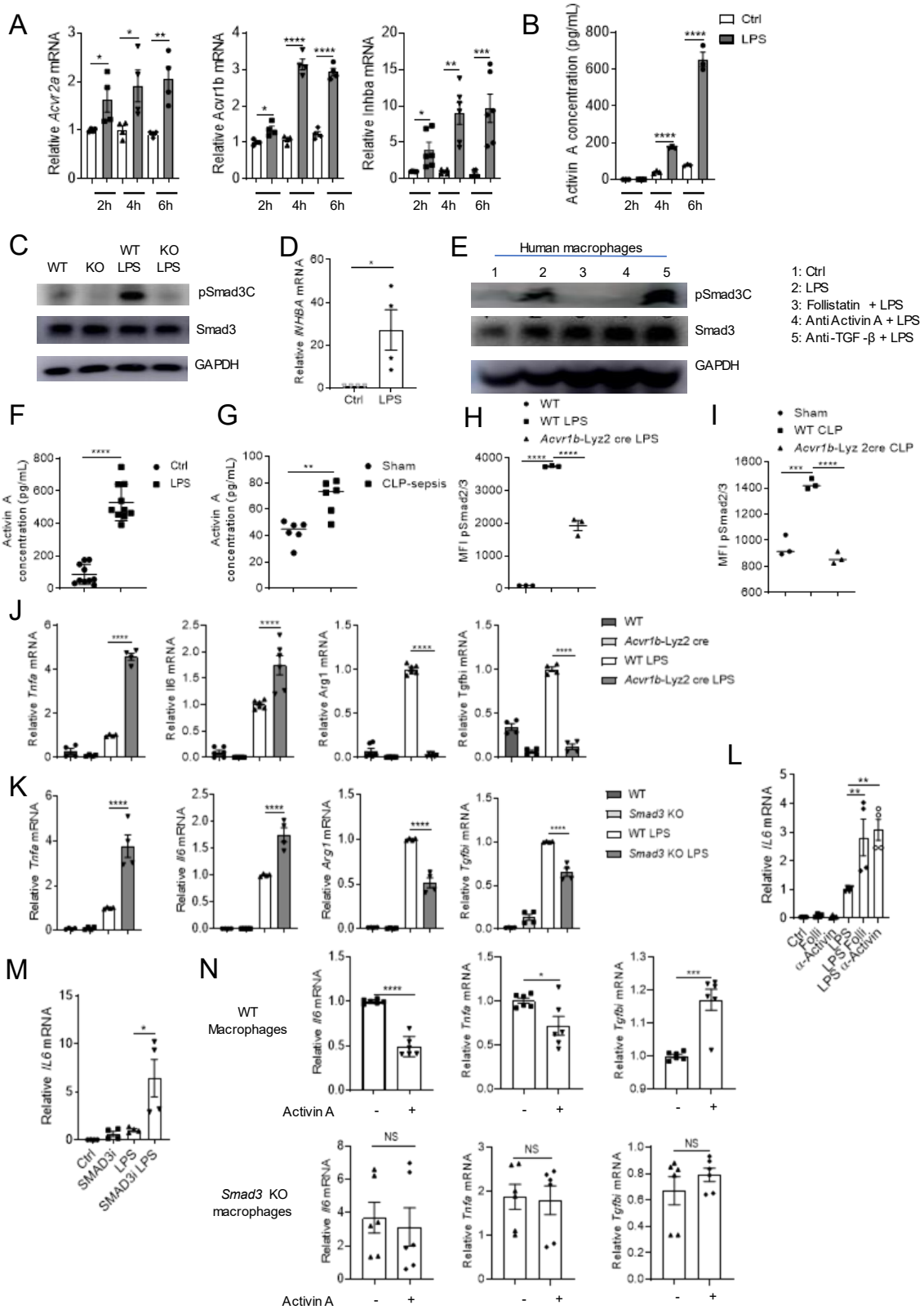
A
Relative Acvr2a mRNA
Relative Acvr1b mRNA
Relative Inhba mRNA
2h
4h
6h
B
Activin A concentration (pg/mL)
Ctrl
LPS
C
WT
KO
WT LPS
KO LPS
pSmad3C
Smad3
GAPDH
D
Relative INHBA mRNA
Ctrl
LPS
E
Human macrophages
1
2
3
4
5
pSmad3C
Smad3
GAPDH
1: Ctrl
2: LPS
3: Follistatin + LPS
4: Anti Activin A + LPS
5: Anti-TGF -β + LPS
F
Activin A concentration (pg/mL)
Ctrl
LPS
G
Activin A concentration (pg/mL)
Sham
CLP-sepsis
H
WT
WT LPS
Acvr1b-Lyz2 cre LPS
MFI pSmad2/3
I
Sham
WT CLP
Acvr1b-Lyz 2cre CLP
MFI pSmad2/3
J
Relative Tnfa mRNA
Relative Il6 mRNA
Relative Arg1 mRNA
Relative Tgfbi mRNA
WT
Acvr1b-Lyz2 cre
WT LPS
Acvr1b-Lyz2 cre LPS
K
Relative Tnfa mRNA
Relative Il6 mRNA
Relative Arg1 mRNA
Relative Tgfbi mRNA
WT
Smad3 KO
WT LPS
Smad3 KO LPS
L
Relative IL6 mRNA
Ctrl
Follii
α-Activin
LPS
LPS Follii
LPS α-Activin
M
Relative IL6 mRNA
Ctrl
SMAD3i
LPS
SMAD3i LPS
N
WT Macrophages
Relative Il6 mRNA
Relative Tnfa mRNA
Relative Tgfbi mRNA
Activin A
Smad3 KO macrophages
NS

953

Figure 3 LPS induces the Activin A-Smad3 axis through a TLR4-Myd88-MAPK-STAT5 pathway

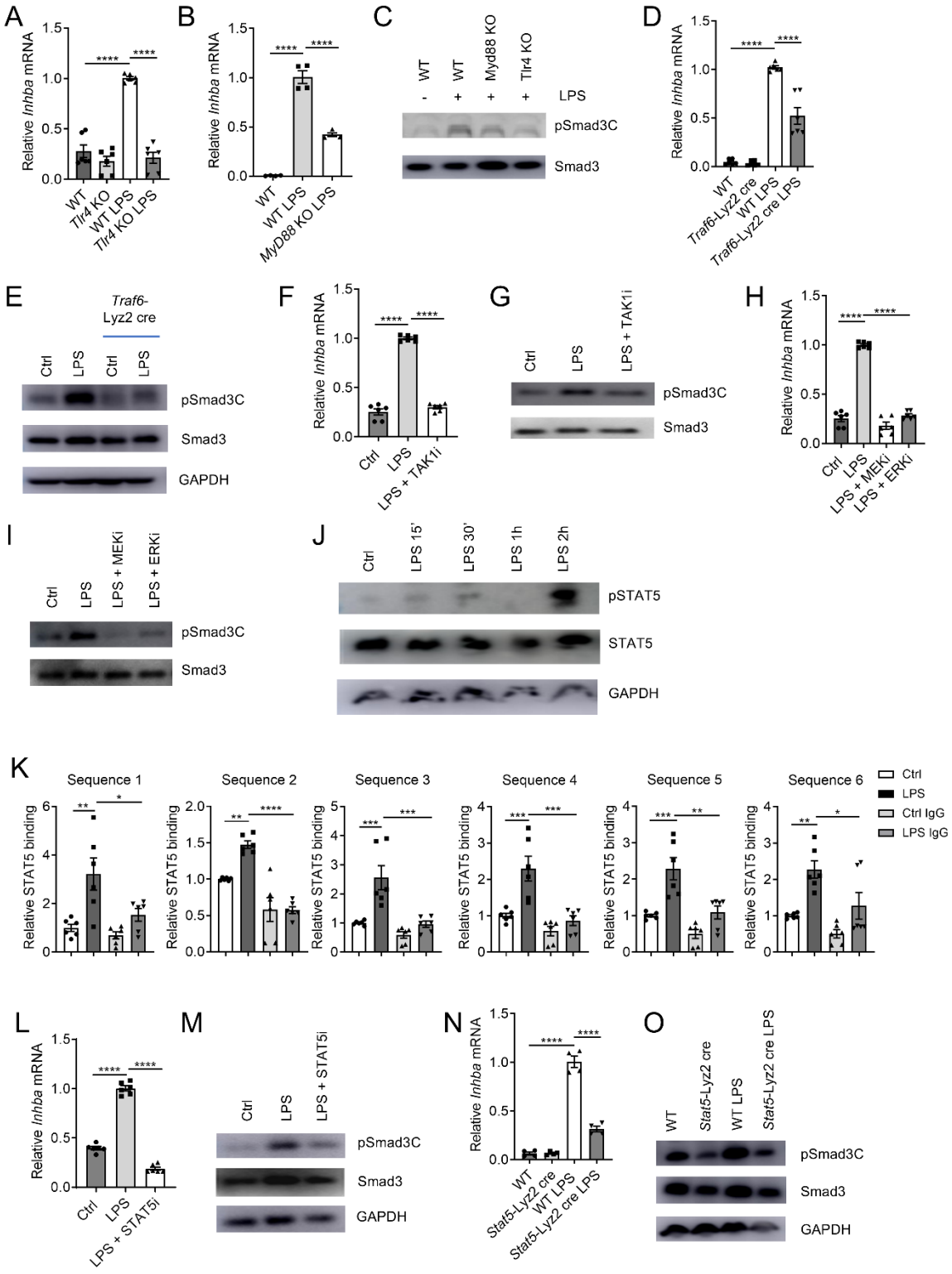

956

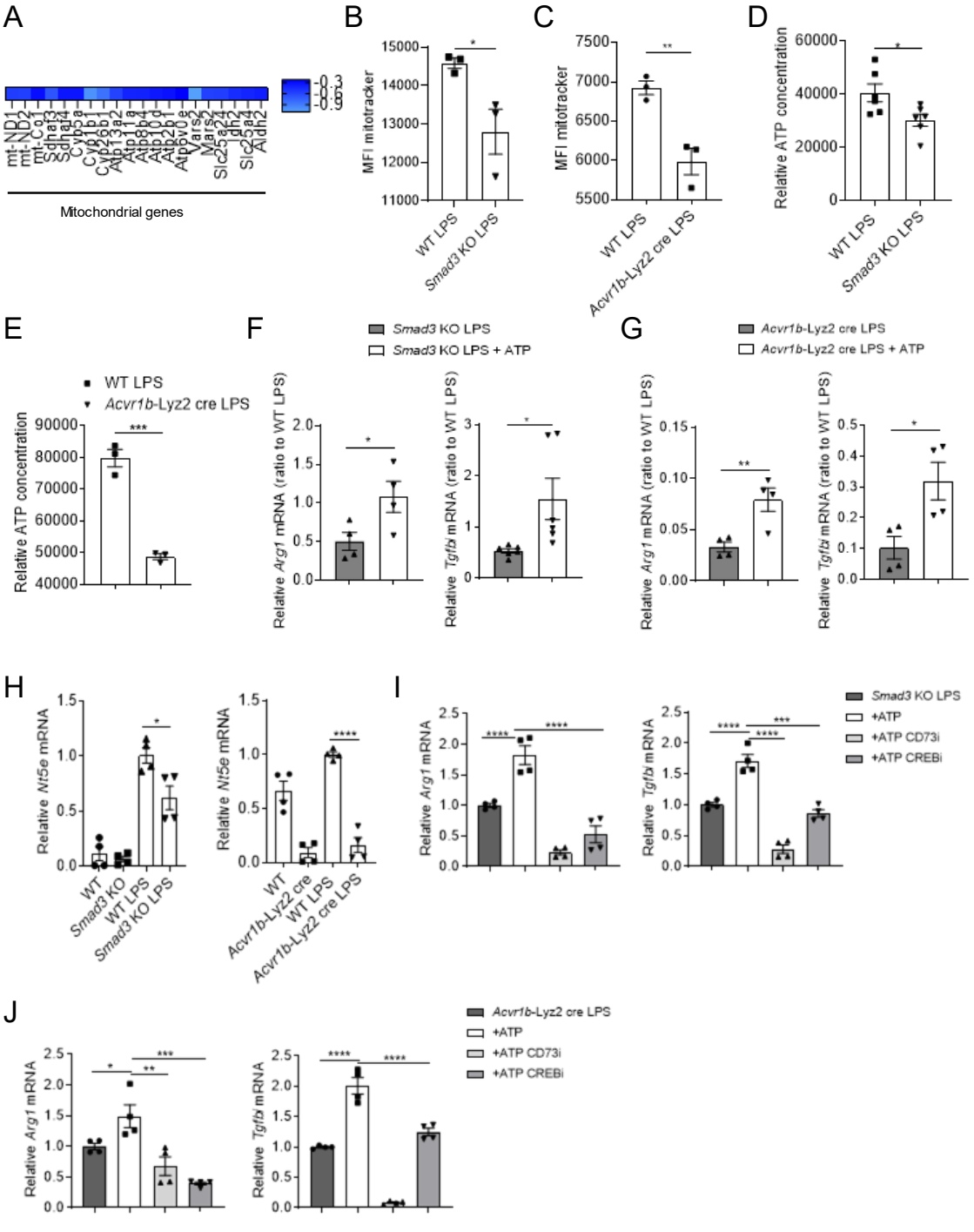
A
B
C
D
E
F
G
H
I
J
Mitochondrial genes
MFI mitotracker
Relative ATP concentration
WT LPS
Smad3 KO LPS
Acvr1b-Lyz2 cre LPS
Smad3 KO LPS + ATP
Acvr1b-Lyz2 cre LPS + ATP
Relative Arg1 mRNA (ratio to WT LPS)
Relative Tgfbi mRNA (ratio to WT LPS)
Relative Nt5e mRNA
Relative Arg1 mRNA
Relative Tgfbi mRNA
+ATP
+ATP CD73i
+ATP CREBi

960

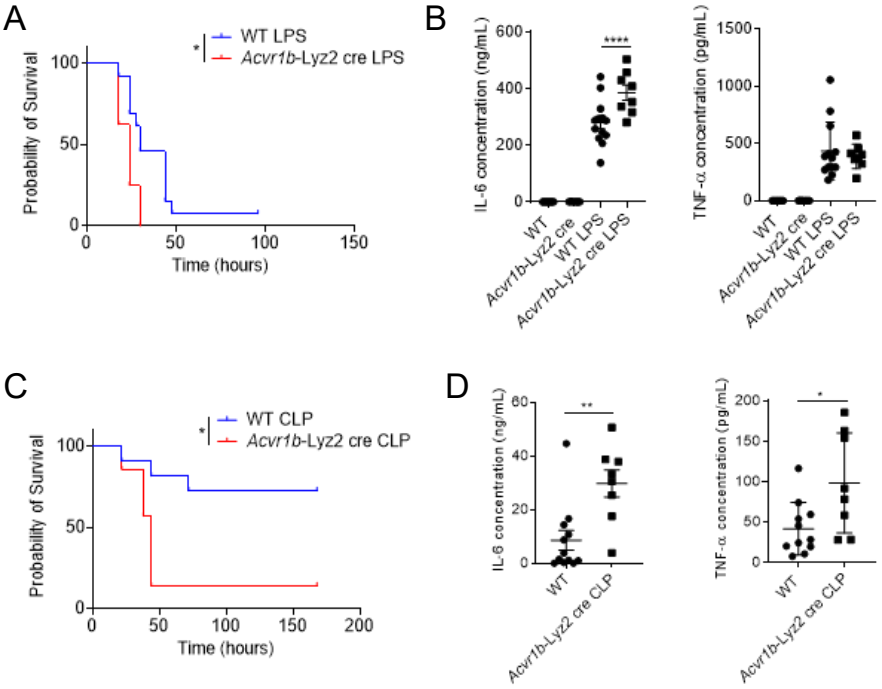
A
WT LPS
Acvr1b-Lyz2 cre LPS
*
Probability of Survival
Time (hours)
B
IL-6 concentration (ng/mL)
TNF-α concentration (pg/mL)
****
WT
Acvr1b-Lyz2 cre
WT LPS
Acvr1b-Lyz2 cre LPS
C
WT CLP
Acvr1b-Lyz2 cre CLP
D
**
*

963

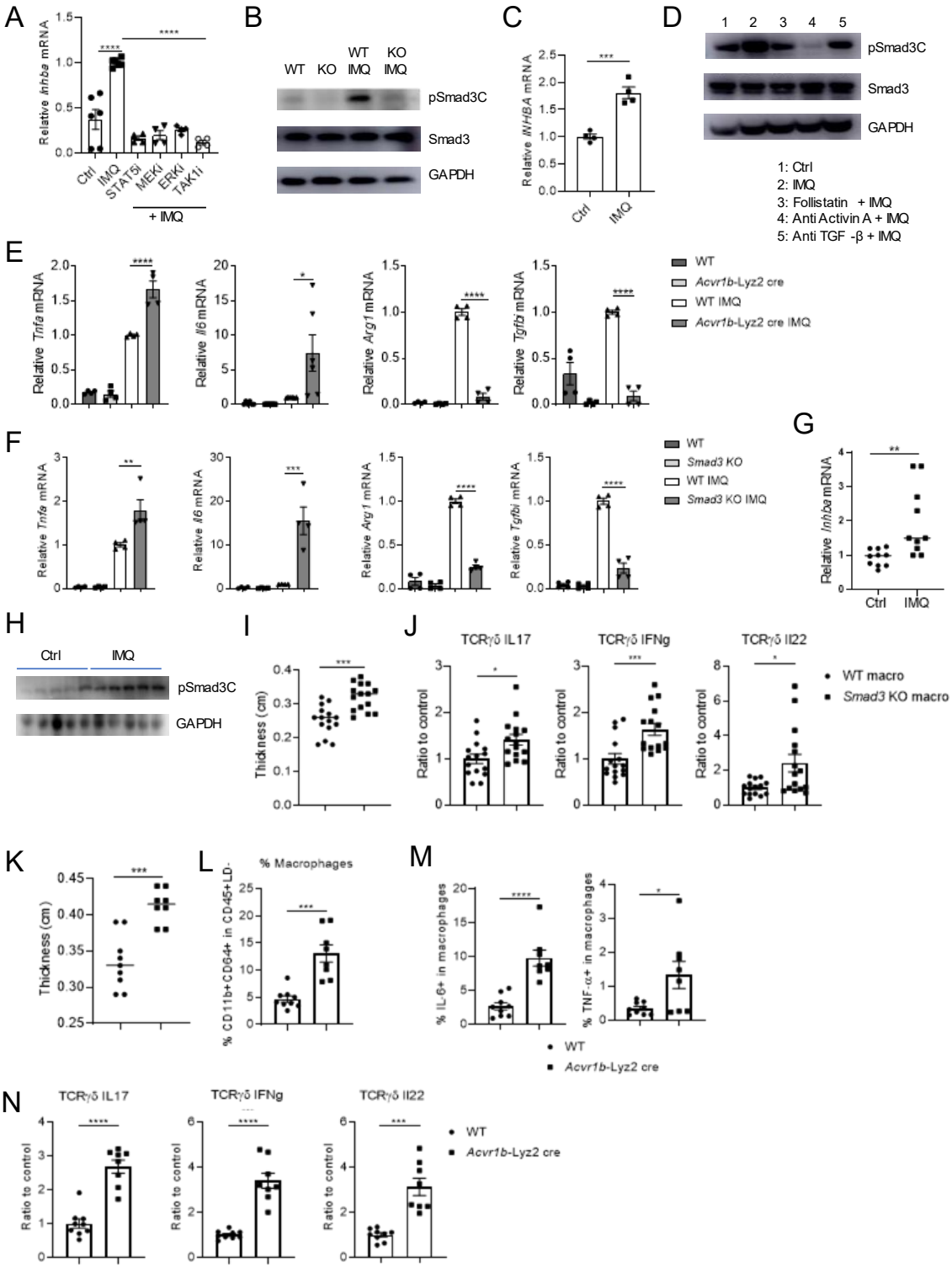
A
Relative Inhba mRNA
Ctrl
IMQ
STAT5i
MEKi
ERKi
TAK1i
+ IMQ
B
WT
KO
WT IMQ
KO IMQ
pSmad3C
Smad3
GAPDH
C
Relative INHBA mRNA
Ctrl
IMQ
D
1 2 3 4 5
pSmad3C
Smad3
GAPDH
1: Ctrl
2: IMQ
3: Follistatin + IMQ
4: Anti Activin A + IMQ
5: Anti TGF -β + IMQ
E
Relative Tnfa mRNA
Relative Il6 mRNA
Relative Arg1 mRNA
Relative Tgfbi mRNA
WT
Acvr1b-Lyz2 cre
WT IMQ
Acvr1b-Lyz2 cre IMQ
F
Relative Tnfa mRNA
Relative Il6 mRNA
Relative Arg1 mRNA
Relative Tgfbi mRNA
WT
Smad3 KO
WT IMQ
Smad3 KO IMQ
G
Relative Inhba mRNA
Ctrl
IMQ
H
Ctrl
IMQ
pSmad3C
GAPDH
I
Thickness (cm)
J
TCRγδ IL17
TCRγδ IFNg
TCRγδ Il22
Ratio to control
WT macro
Smad3 KO macro
K
Thickness (cm)
L
% Macrophages
% CD11b+CD64+ in CD45+LD-
M
% IL-6+ in macrophages
% TNF-α+ in macrophages
WT
Acvr1b-Lyz2 cre
N
TCRγδ IL17
TCRγδ IFNg
TCRγδ Il22
Ratio to control
WT
Acvr1b-Lyz2 cre

966